Test Plan - Impact Test of a General Aviation Composite Airframe

Steven J. Hooper
J. B. Dwerlkotte Assoc., Inc.

Todd R. Hurley
Simula Technologies, Inc.
Phoenix, AZ

Richard L. DeWeese
FAA Civil Aeromedical Institute
Oklahoma City, OK

Report Reference Number: AGATE-WP3.4-034026-080, Rev A
Work Package Title: WBS3.0 Integrated Design and Manufacturing
Date of General Release: February 1, 2002

TABLE OF CONTENTS

Figures

Tables

1. INTRODUCTION

AGATE work package 3.4, the Advanced Crashworthiness Group (ACG), is planning a series of four light airplane drop tests at the NASA Impact Dynamics Research Facility for the purpose of improving the crashworthiness of general aviation aircraft by employing a systems approach in their design and certification. The program considers the crashworthy performance of these aircraft, which impact both concrete and soil surfaces.

The AGATE JSRA members participating in the Advanced Crashworthiness Group include: Simula Technologies, Inc., The Lancair Company; Mod Works, Inc.; FAA; Wichita State University; NASA Langley Research Center; and Cessna Aircraft Company.

Only one test is currently planned under the AGATE program and it will be onto a hard surface as described below. The other tests will be conducted after the conclusion of the AGATE program if funding becomes available. This test plan covers only the AGATE test.

2. BACKGROUND

The AGATE Advanced Crashworthiness Group is conducting a program, referred to as “Crashworthy Airplane” in which the group is designing, fabricating, and crash testing a next-generation single-engine, four-place, composite airplane. This program is also developing a Systems Approach to whole-airplane crashworthy design and certification. Originally, this task was referred to as “Path B”.

Both programs utilize the lessons learned in the Terry Engineering SBIR crash tests to develop production airplanes, which possess certifiable crashworthy performance. Data gathered from the Crashworthy Airplane test series will be used to evaluate the efficacy of the Systems Approach to Crashworthiness and to improve the design process if deficiencies are discovered. Eventually, the scope of the Systems Approach to Crashworthiness will be broadened to include other airframe configurations and thus improve the crash safety of the general aviation fleet.

Data acquired during the full-scale dynamic tests will also be used to validate the results predicted by the computer models, which are used to integrate the various crashworthy technologies represented in the design of the AGATE airplane.

3. OBJECTIVES

The objective of the first drop test is to impact the AGATE airplane onto a concrete surface at Vso (57 kts), -30º impact angle, -30º pitch, no roll, and no yaw. Data will be collected regarding the airframe structural response, seat performance, restraint performance, and occupant responses. These data will be used to evaluate the crashworthiness of the AGATE airplane (airframe, seats, restraints, interior) as well as to evaluate the Systems Approach to Crashworthy design. Particular attention will be paid to the performance of the engine mount and subfloor, and to the transient deformation and structural integrity of the aircraft cabin.

4. TEST DESCRIPTION

4.1 Test Facility

The tests will be performed at NASA Impact Dynamics Research Facility (IDRF) at the Langley Research Center in Hampton, VA (Fig. 1). This facility has been developed to crash test full-scale general aviation aircraft under free flight conditions. A pendulum swing method from a large gantry is used to obtain desired flight paths. Flight paths up to –60º and aircraft velocities along the flight paths up to about 88.6 ft/s (60.4 mph or 52.5 knots) have been obtained with a combination of swing-cable lengths and release heights made available by the gantry. Higher flight path velocities have been achieved in a few tests by using rocket augmentation. Test parameters at the IDRF are controllable with flight-path angles accurate within 8 percent, aircraft velocity accurate within 6 percent, pitch angles accurate to 4.25º, and roll and yaw angles acceptable under wind velocities up to 14.76 ft/s (approx. 10 mph).

The test described in this document will require a higher velocity (57 knots) than prior gravity-only tests. NASA IDRF personnel have calculated that this velocity can be achieved without augmentation.

4.2 Test Article

The test article will be low wing, four place, all composite, fixed gear airplane supplied by Lancair, an AGATE ACG member. See Figs. 2 & 4. The test specimen will be built to prototype or production drawings and will be conformed and documented by the ACG prior to the test. Structural damage to the test article will be evaluated after the test to determine the feasibility of repair and reuse in subsequent tests.

The test article consists of the following:

- Fuselage and empennage. The fuselage is fabricated specifically for this test and contains a number of features that vary significantly from the production version of this airplane. These features include occupant compartment structure that is sized for the expected crash loads, an energy absorbing subfloor, and structural details to prevent plowing on soil. The landing gear will not be installed on the aircraft for the test and may or may not be available for ground support, so a dolly could be needed. The rudder and elevator will not be installed on the test article.
- Doors. The stock doors will be used. The latching pins and handles may also be production items or may be test-only items with equivalent function. Weather stripping may be installed, but is not required for the test.
- Wing. The wing will be essentially stock, but will not have any control surfaces, flaps, or linkages. Fuel tanks and fuel transfer lines to the fuselage will be included, but may be different from the production components.
- Engine and mount. The engine will be a stock, but inoperable Continental IO550 six-cylinder horizontally opposed engine. Ballast will be attached to represent the propeller and accessories. The mount will be an energy absorbing design specific to this test.
- Cowl. The cowl design for the drop test article is based on the production model, but is modified to increase its puncture and tear resistance.

- Seats and restraints. The current plan is to use the stock seats and restraints from the production model. Cloth, rather than leather, dress covers will be used due to cost considerations.
- Interior components. Instrument panel, armrests, center console, and trim will be installed in the fuselage as required. These components may be production parts or mockups.

Fittings will be installed on the airframe to provide attachment locations to the NASA IDRF. The design of this mounting hardware will be very similar to the hardware used in the Terry tests, shown in Figs. 5-7.

Some aircraft equipment and components will not be included in the test article. Ballast may be used in place of the control surfaces, control linkages, propeller, landing gear, and other accessories as necessary. Ballast will be added to the wing attachment fittings to adjust the weight of the test article, including ATD's, to approximately 3200 pounds. Ballast shall be installed in the test article to position the aircraft's center of gravity to a point that is within the cg limits as described in the Pilot's Operating Handbook for the Lancair 300. The location and weight of all items of mass will be documented prior to the test. Furthermore, the test director will review and approve the installation of each item of mass prior to the test.

Coordination between the test director, Steve Hooper, the test article manufacturer, Lancair, the test preparation group at the NASA IDRF, and the ACG Workpackage Leader, SIMULA, is required to insure proper integration of the crashworthiness technologies.

4.3 Test Conditions

The Path B test conditions were established during deliberations of the AGATE ACG and are summarized below. They are similar to those used in previous NASA IDRF light airplane tests, the conditions used in the Terry tests, and the results of AGATE Metrics program. The test will be conducted on a concrete impact surface at the following conditions:

- 57 knots impact velocity (a representative Vso for the AGATE aircraft)
- -30° Flight path angle
- -30° pitch (nose down)
- 0° roll
- 0° yaw

4.4 Instrumentation

The instrumentation can be classified in three groups of transducers, which will be used to measure the performance of the airframe, seats and restraints, and occupants. The location, number, and type of instrumentation are presented in Table 1 of this report. The locations of these transducers are also shown in Figs. 8-10. The airframe accelerometer locations will be determined by the Test Director, Steve Hooper; the FAA National Resource Specialist for Crashworthiness, Steve Soltis; and the NASA Engineer in charge of this project, Karen Lyle. Members of this group will solicit input from ACG members regarding special instrumentation requirements associated with the various crashworthiness technologies contained in the test article.

4.5 Anthropomorphic Test Devices (ATD's)

Four instrumented Hybrid II (49 CFR Part 572, Subpart B) ATD's will be installed in the test article.

4.6 Data Acquisition

Data from the instruments will be acquired at 10,000 samples per second and will be stored as raw, unfiltered signals. The test data will be filtered at 4 kHz with an analog anit-aliasing filter. The data will then be filtered post-acquisition per SAE J211 and SAE AS8049 Rev A requirements. IDRF personnel and the principle investigator will assign an appropriate filter class to each channel of data. The instrumentation tables will include the assigned channel filter class.

4.7 Photographic Coverage

The test will be documented with both still and motion photography. NASA Langley personnel will be responsible for the photo documentation.

4.7.1 Still Photography

NASA photographers will be responsible for documentation photographs. Pretest photos will be taken to document the instrumentation installed in the test article, the onboard experiments, the test setup, and the impact area. Posttest photos will be taken of the test specimen with overall and close-up views of damaged areas, the onboard experiments, and the impact area.

4.7.2 Motion Pictures

The crash test shall be documented with both high-speed and real-time cameras. The AGATE ACG and NASA IDRF shall determine the exact number and location of the cameras prior to the test.

High-speed cameras shall be either 16mm film or equivalent resolution digital video. Frame rates of these cameras shall be 400 frames per second. Three or more high-speed ground cameras will be used to document the event from different angles. The camera's field of view would cover the airplane motion from just before impact, through the impact and rotation, and into the first part of the slide-out. Markers would be placed on the fuselage and tracked to measure rigid-body motion, transient fuselage bending and deformation, and permanent global deformations. The Photometric data will be collected and analyzed per SAE J211 guidelines.

At least one real-time video camera shall also be used to document the event. This camera shall record broadcast-quality video. The location of this camera will also be determined the NASA engineer and the Test Director. Due to the potential sensitivity of this test to Lancair, the maker of the test article, only NASA LaRC personnel will be allowed to take movies or video during the test.

4.7.3 Camera Synchronization Device

The purpose of the synchronization device is to provide a common time reference for the data acquisition system, film cameras and video cameras that are used to record the results of a test. The device consists of a bright light source, a light sensor, an electronics box, a strobe light and interconnecting cabling. As shown in Fig. 11, the light source is placed on the near side and the sensor is placed on the far side of the impact area. They are positioned such that the subject passes between them soon after the impact event begins. The light source and sensor both have tubular shields to reduce glare, and therefore must be precisely aligned with one another. The strobe light is placed on the near side in the field of view of all cameras (if possible). When fired, it is visible from both the horizontal and vertical directions.

The electronic box generates several signals when the light beam is broken. A high/low 5V TTL signal is sent to the video camera for event marking or triggering. A low/high/low 5V TTL pulse, of 60 ms duration, is sent to the data acquisition system to be recorded on a data channel. The box provides a dedicated 400V, 1.5A, SCR switch closure for the strobe to fire it. An additional isolated 125V, 1A, relay switch closure of 60 ms duration is also available to trigger an additional video camera. All TTL signals and switch closures occur within 50 microseconds of the light beam being broken. The strobe becomes visible 1 millisecond after the trigger signal is generated, and remains bright for a total of 3 milliseconds. Fig. 12 shows how the various components are connected to the electronics box.

4.7.4 Photometric Camera Alignment

In order to derive accurate position data from the film or video of the test, all cameras used for this purpose must be aligned with their optical axis perpendicular to the plane of motion of the subject. Fig. 11 shows the orientation of these "photometric cameras", and the required Field of View (FOV). This figure also illustrates how the reference length targets should be placed in the foreground of the image.

5. GENERAL INFORMATION

5.1 Test Attendees

The ACG has not decided whether the test shall be restricted and, if so, who shall attend. If the test is restricted, the ACG will provide a list of attendees to NASA IDRF. This will be determined in early 2001.

5.2 Photographic Privilege

Except for NASA LaRC personnel who are documenting the test, ACG test participants who wish to take pre- and post-test still photographs must get permission from the Test Director. A list of attendees with photographic privileges will be provided to NASA IDRF prior to the test.

5.3 Pre-Test Responsibilities

A procedural checklist will be included in a future revision of this test plan. The checklist will describe the pre-test procedure leading up to the test and who has responsibility for each experiment on the test article.

5.4 Pre-Test Briefing

NASA IDRF will conduct a pre-test briefing to review the test with the attendees.

5.5 Post-Test Data Distribution

The data and still photos collected by the NASA IDRF will be given to the Test Director who will be responsible for their distribution. These data will only be distributed to the AGATE ACG members directly involved in the test. The data will be distributed on a CD or ZIP disk in an ASCII format that is defined by NASA IDRF personnel.

The Test Director will write the test report with input and assistance from the involved ACG members. These members will review the test report before it is finalized. The test report will be distributed to all ID&M principle members, upon request, only after the report has been released by the ACG.

5.6 Show Stoppers

Late arrival of the test specimens

Weather

5.7 Pass-Fail Criteria

Maintenance of Occupant Space

Limits for Occupant Loads

5.8 Safety

All AGATE participants will follow the NASA IDRF safety procedures.

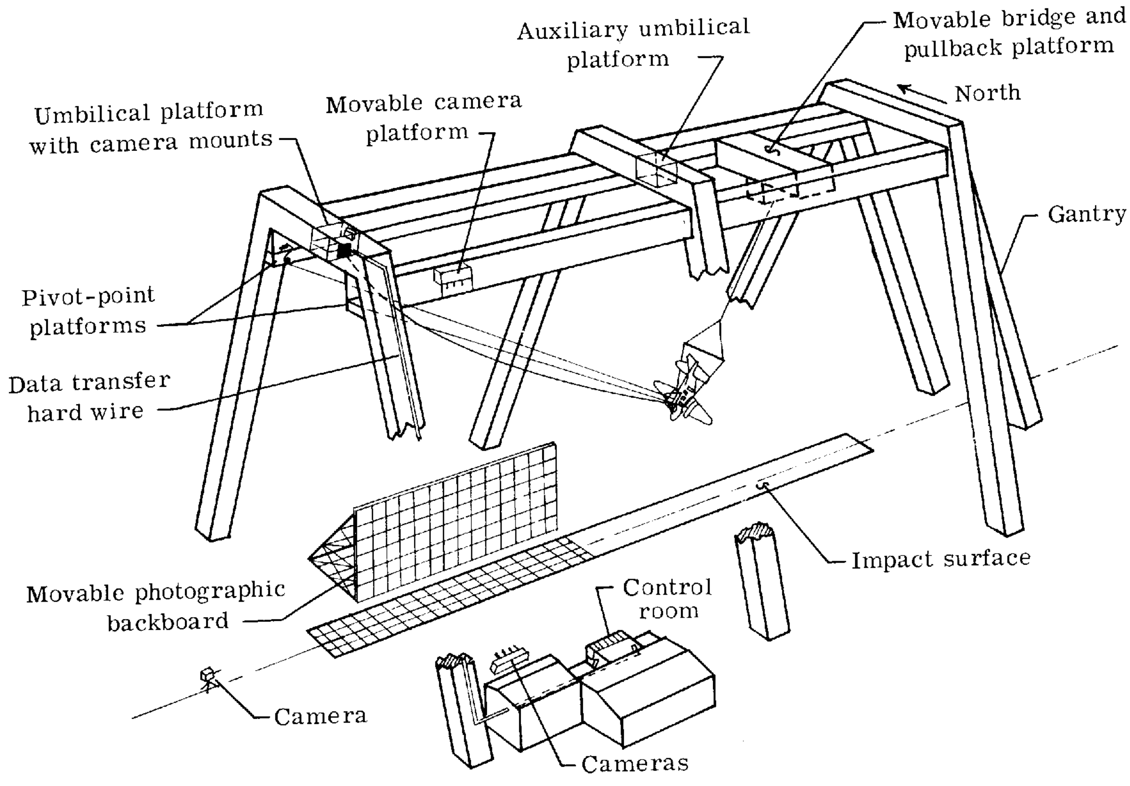

Diagram of impact dynamics research facility.

Figure 1 – Diagram of Impact Dynamics Research Facility

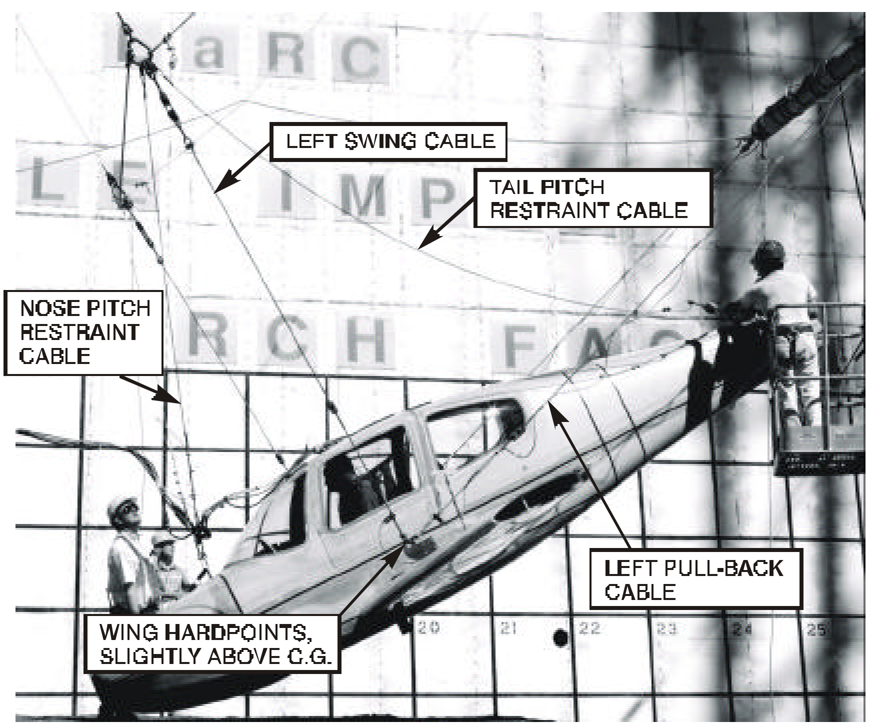

Figure 2 – Swing Harness Configuration on Test Article

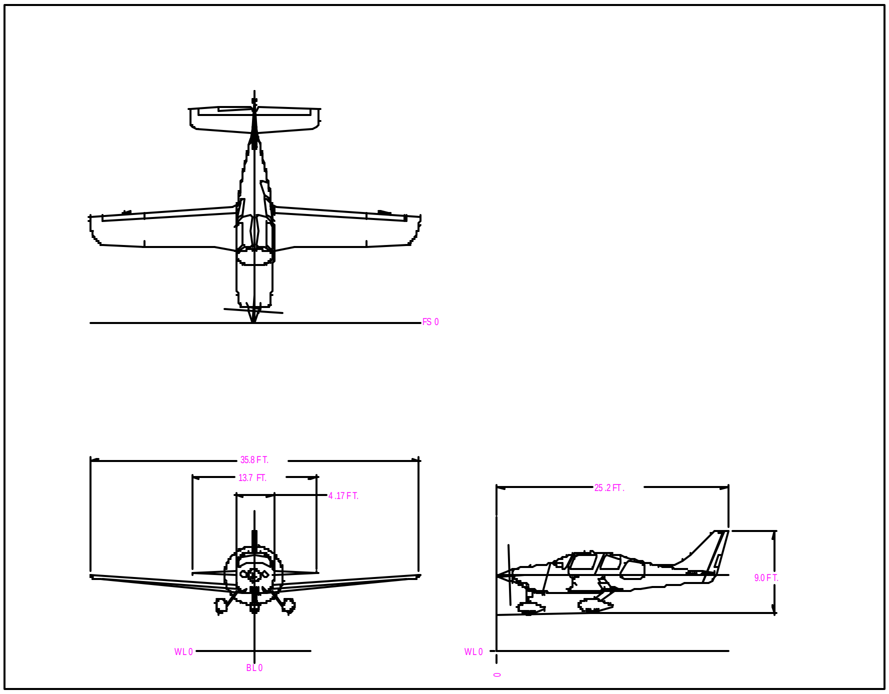

Figure 3 – Lancair Aircraft Three-View Drawing

Figure 4 – Lancair Aircraft

Figure 5 – Top View of Test Article

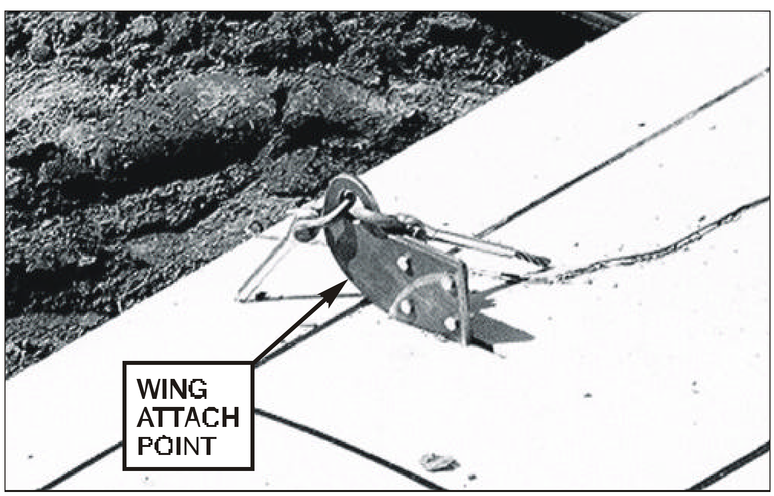

Figure 6 – Close-Up View of Wing Cable Mounting Bracket

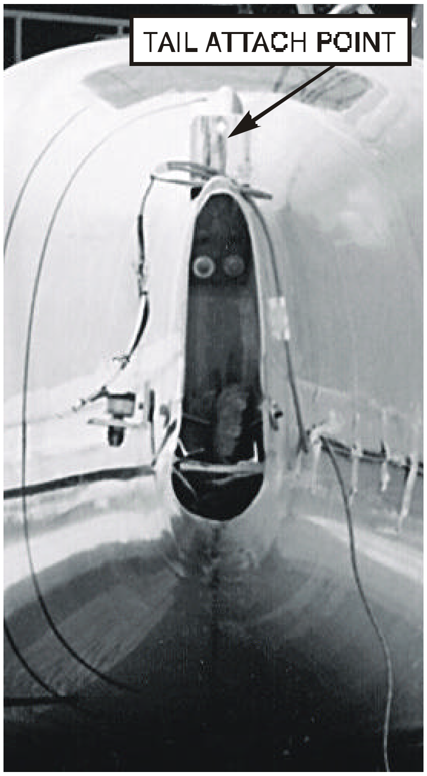

Figure 7 – Tail Mounting Hardware

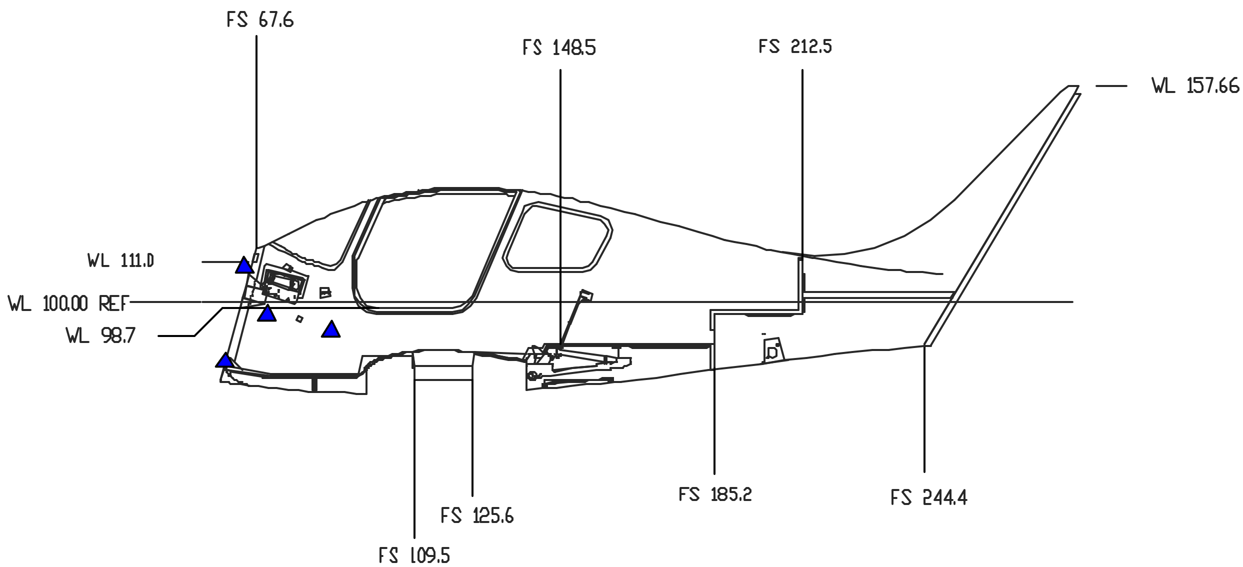

Figure 8 – Fuselage Side View Instrumentation Location Schematic

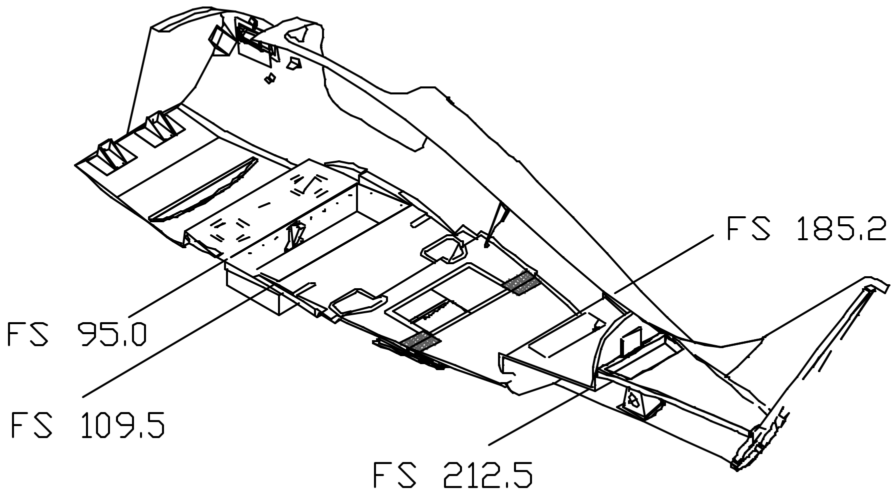

Figure 9 – Fuselage Isometric View Instrumentation Location Schematic

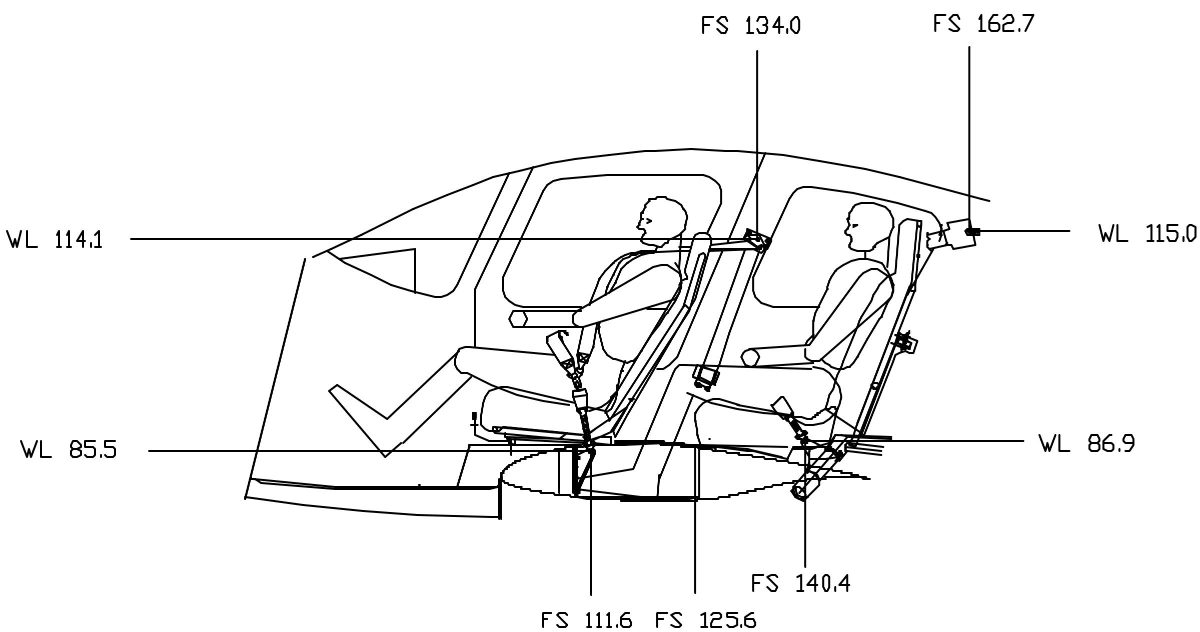

Figure 10 – Seat and Restraint System Installations

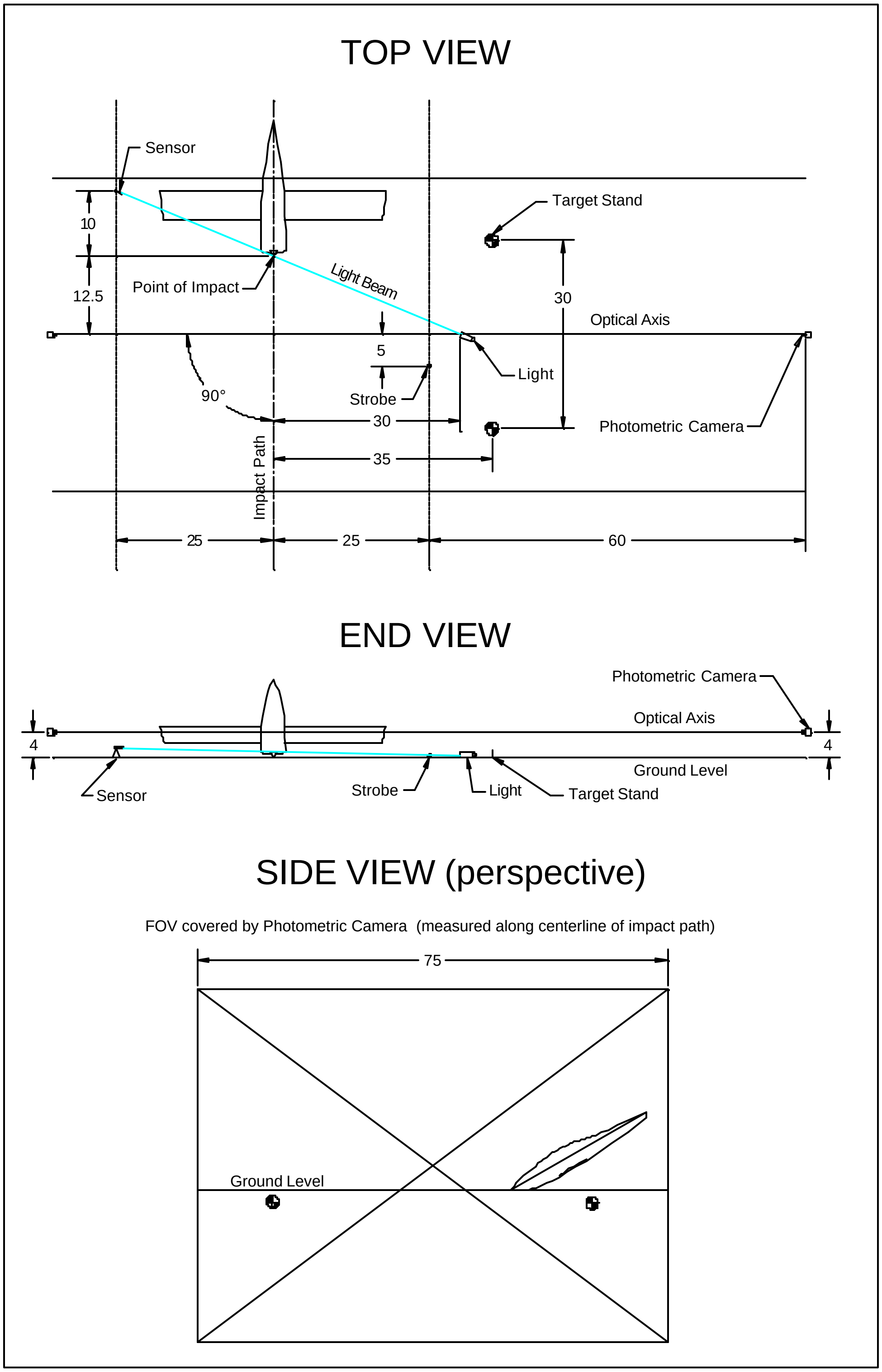

Figure 11 – Photometrics Layout

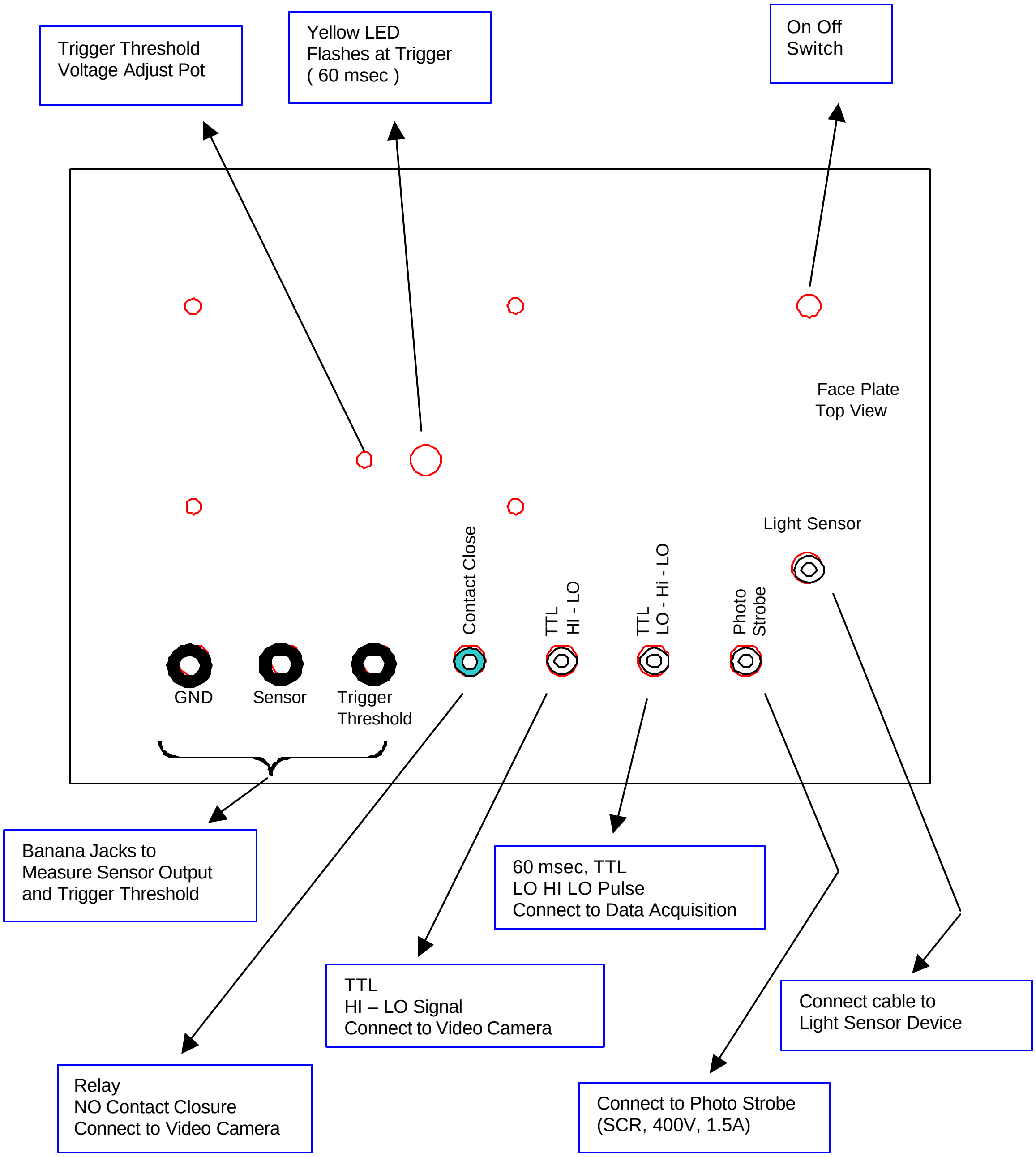

Figure 12 – Photometrics Control Unit

Table 1 - Accelerometer Locations

Sensor Location	Data		Range		FS	BL	WL
	Ch	Min	Max	Units			
Pelvis_Pilot_z	1	-200	200	G			
Head_Pilot_x	2	-100	100	G			
Head_Pilot_y	3	-100	100	G			
Head_Pilot_z	4	-200	200	G			
Lumbar_Load_Pilot	5	-3500	3500	lb			
Upper_Torso_Restraint_Pilot	6	-3000	3000	lb			
Lower_Eng_Mt_LHS_x	7	-750	750	G	58.0	7.0	90.0
Lower_Eng_Mt_LHS_z	8	-750	750	G	58.0	7.0	90.0
Pelvis_LHS_Pax_z	9	-200	200	G			
Head_LHS_Pax_x	10	-100	100	G			
Head_LHS_Pax_y^	11	-100	100	G			
Head_LHS_Pax_z	12	-200	200	G			
Lumbar_Load_LHS_Pax	13	-3500	3500	lb			
Upper_Torso_Restr_LH_Pax	14	-3000	3000	lb			
Upper_Eng_Mt_LHS_x	15	-750	750	G	63.0	21.0	105.0
Upper_Eng_Mt_LHS_z	16	-750	750	G	63.0	21.0	105.0
Pilot_St_Trk_Aft_IB_z	17	-750	750	G	108.0	5.0	86.0
Pilot_St_Trk_Aft_OB_z	18	-750	750	G	108.0	15.0	86.0
Pilot_St_Trk_Fwd_IB_x	19	-750	750	G	98.0	15.0	86.0
Pilot_St_Trk_Fwd_OB_z	20	-750	750	G	98.0	15.0	86.0
Pilot_St_Trk_Fwd_IB_z	21	-750	750	G	98.0	5.0	86.0
Engine_Fwd_x	22	-750	750	G	25.0	5.0	98.0
Engine_Fwd_z	23	-750	750	G	25.0	5.0	98.0
Sidewall_LHS_1_x	24	-750	750	G	75.0	22.0	96.0
Sidewall_LHS_1_z	25	-750	750	G	75.0	22.0	96.0
Sidewall_LHS_2_x	26	-750	750	G	85.0	22.0	93.0
Sidewall_LHS_2_z	27	-750	750	G	85.0	22.0	93.0
Rear_Engine_x^	28	-750	750	G	54.0	3.0	106.0
Rear_Engine_z	29	-750	750	G	54.0	3.0	106.0
	30						
Camera_Switch	31	-5	5	V			
Test Signal	32	-2	2	V			

Table 1 - Accelerometer Locations (cont.)

Sensor Location	Data		Range		FS	BL	WL
	Ch	Min	Max	Units			
Pelvis_CoPilot_z	33	-200	200	G			
Head_CoPilot_x	34	-100	100	G			
Head_CoPilot_y	35	-100	100	G			
Head_CoPilot_z	36	-200	200	G			
Lumbar_Load_CoPilot	37	-5000	5000	lb			
Upper_Torso_Restr_CoPilot	38	-3000	3000	lb			
Lower_Eng_Mt_RHS_x	39	-750	750	G	58.0	-7.0	90.0
Lower_Eng_Mt_RHS_z	40	-750	750	G	58.0	-7.0	90.0
Pelvis_RHS_Pax_z	41	-200	200	G			
Head_RHS_Pax_x	42	-100	100	G			
Head_RHS_Pax_y	43	-100	100	G			
Head_RHS_Pax_z	44	-200	200	G			
Lumbar_Load_RHS_Pax	45	-5000	5000	lb			
Upper_Torso_Restr_LH_Pax	46	-3000	3000	lb			
Upper_Eng_Mt_RHS_x	47	-750	750	G	63.0	-21.0	105.0
Upper_Eng_Mt_RHS_z	48	-750	750	G	63.0	-21.0	105.0
CoPilot_St_Trk_Aft_IB_z	49	-750	750	G	108.0	-5.0	86.0
CoPilot_St_Trk_Aft_OB_z	50	-750	750	G	108.0	-15.0	86.0
CoPilot_St_Trk_Fwd_IB_x	51	-750	750	G	98.0	-15.0	86.0
CoPilot_St_Trk_Fwd_OB_z	52	-750	750	G	98.0	-15.0	86.0
CoPilot_St_Trk_Fwd_IB_z	53	-750	750	G	98.0	-5.0	86.0
Tail_Cone_y	54	-200	200	G	212.0	0.0	103.0
Tail_Cone_z	55	-750	750	G	212.0	0.0	103.0
Sidewall_RHS_1_x	56	-750	750	G	75.0	-22.0	96.0
Sidewall_RHS_1_z	57	-750	750	G	75.0	-22.0	96.0
Sidewall_RHS_2_x	58	-750	750	G	85.0	-22.0	93.0
Sidewall_RHS_2_z	59	-750	750	G	85.0	-22.0	93.0
	60						
	61						
DAS Accel	62	-200	200	G			
Radar	63	-2	2	V			
Test Signal	64	-2	2	V			

Appendix A – Stress Analysis of Data Acquisition System Installation

The following analysis is performed to verify the structural integrity of the installation of the data acquisition system. It is prepared by loading condition, checking in each condition the items having the greatest loads, moments and stresses, thereby substantiating the remainder of the installation by comparison. The installation consists of a number of data acquisition units that are each attached to a 0.090-in. thick 6061-T6 aluminum mounting plate by at least four number ten steel screws. Each of these screws conservatively possesses shear and tensile strengths of 992[1] lb. and 994[2] lb. respectively. The 30-lb. battery installations are critical since they are the heaviest and possess the highest centers of gravity, which is assumed to be 3.0 in. above the base. They are conservatively considered to be retained by four, number ten steel screws. The strength of these fasteners is analyzed using the interactive failure theory presented in Bruhn[3] and summarized as

$$Rt^2 + Rs^2 = 1$$
$$Rt = F / f$$
$$Rs = F_s / fs$$
$$MS = 100\left[\frac{1}{\sqrt{Rt^2 + Rs^2}} - 1\right]$$

where F and F_s respectively represent the tensile and shear loads resisted by the fastener, and respectively f and f_s represent the tensile and shear strengths of the fastener.

The tension force F produced in these fasteners during the 50g forward load condition are evaluated as

$$\begin{aligned} F &= (30\ lb.)(50)(3\ in.) / ((4\ in.)(2)) \\ &= 562.5\ lb. \end{aligned}$$

The shear force F_S, is evaluated as

$$\begin{aligned} F_s &= (30\ lb.)(50) / (2) \\ &= 375\ lb. \end{aligned}$$

[1] Table 8.1.5(a) MIL-HDBK-5F, Nov. 1990
[2] Table 8.1.5(b_1) MIL-HDBK-5F, Nov. 1990
[3] Bruhn, E.F., *Analysis & Design of Flight Vehicle Structures*, Tri-State Offset Company, Cincinnati, OH, 1973.

The margin of safety is subsequently evaluated as

$$MS = 100\left[\left[\left(\frac{562.5}{994}\right)^2 + \left(\frac{375}{992}\right)^2\right]^{-1/2} - 1\right]$$
$$= 46.9\,\%$$

Thus the most critical fasteners possess a large positive margin of safety for the 50g forward load and are satisfactory for the forward load condition.

These fasteners are also analyzed for a 10g upload condition. The fastener load is calculated as

$$F = (30\ lb.)(10)/\ 4$$
$$= 75\ lb.$$

The corresponding margin of safety is calculated as

$$MS = 100\left[\frac{994\ lb.}{75\ lb.} - 1\right]$$
$$= 1225\ \%$$

Thus the fasteners are more than adequate to resist a 10g upload. Note the data acquisition units bear against the floor of the baggage compartment during the download condition. Thus, for this condition, they are satisfactory by inspection.

The mounting plate was bonded to the outside perimeter of the baggage compartment with Hysol EA 9309.3NA adhesive, which develops 4200-psi shear and 4500-psi tensile strengths. Two load conditions were considered: A 50-G download and a 10-G forward load. The interface loads were calculated using a rigid body analysis where the adhesive joint was considered to be 28 discrete fasteners, whose locations are specified in Table A.1. Each of these fasteners is conservatively estimated to possess shear and tensile strengths of 4200 lb. and 4500 lb., respectively based on a 1.0 in^2 adhesive area. Examination of the results are presented in Tables A.2 and A.3 reveals very large margins of safety at each location for each load condition.

Table A.1 - Data Acquisition Interface Loads Analysis – Fastener Locations

ATTACH	X	Y	Z
1	0	20.5	0
2	4	19.78	0
3	8	19.06	0
4	12	18.34	0
5	16	17.62	0
6	20	16.9	0
7	24	16.18	0
8	28	15.46	0
9	32	14.74	0
10	34.75	14.245	0
11	37.5	13.75	0
12	0	-20.5	0
13	4	-19.78	0
14	8	-19.06	0
15	12	-18.34	0
16	16	-17.62	0
17	20	-16.9	0
18	24	-16.18	0
19	28	-15.46	0
20	32	-14.74	0
21	34.75	-14.245	0
22	37.5	-13.75	0
23	37.5	-10	0
24	37.5	-6	0
25	37.5	-2	0
26	37.5	2	0
27	37.5	6	0
28	37.5	10	0
Anchor Centroid			
	23.48	0.00	0.00

Table A.2 - 50-G Forward Load - Superposition Solution

	FORWARD LOAD REACTIONS							
ATTACH	X REACT	Y REACT	Z REACT	MS		shear	Rt	Rs
1	201.86	-12.18	77.67	1855.0%		202.2313	0.01726	0.04815
2	202.24	-10.11	64.44	1888.3%		202.49	0.01432	0.048212
3	202.61	-8.03	51.21	1916.1%		202.7703	0.01138	0.048279
4	202.98	-5.96	37.98	1937.4%		203.0721	0.00844	0.04835
5	203.36	-3.88	24.75	1951.8%		203.3953	0.0055	0.048427
6	203.73	-1.81	11.52	1958.6%		203.7398	0.002559	0.048509
7	204.11	0.27	-1.71	1957.8%		204.1055	0	0.048597
8	204.48	2.34	-14.94	1953.9%		204.4923	0	0.048689
9	204.85	4.42	-28.17	1949.8%		204.9001	0	0.048786
10	205.11	5.85	-37.27	1946.9%		205.1926	0	0.048855
11	205.37	7.27	-46.37	1943.8%		205.4949	0	0.048927
12	223.14	-12.18	77.67	1687.8%		223.4683	0.01726	0.053207
13	222.76	-10.11	64.44	1718.5%		222.9916	0.01432	0.053093
14	222.39	-8.03	51.21	1745.3%		222.5339	0.01138	0.052984
15	222.02	-5.96	37.98	1767.4%		222.0952	0.00844	0.05288
16	221.64	-3.88	24.75	1784.5%		221.6757	0.0055	0.05278
17	221.27	-1.81	11.52	1795.8%		221.2756	0.002559	0.052685
18	220.89	0.27	-1.71	1801.4%		220.8948	0	0.052594
19	220.52	2.34	-14.94	1804.5%		220.5335	0	0.052508
20	220.15	4.42	-28.17	1807.4%		220.1919	0	0.052427
21	219.89	5.85	-37.27	1809.4%		219.9684	0	0.052373
22	219.63	7.27	-46.37	1811.2%		219.7543	0	0.052322
23	217.69	7.27	-46.37	1828.3%		217.8097	0	0.051859
24	215.61	7.27	-46.37	1846.8%		215.7356	0	0.051366
25	213.54	7.27	-46.37	1865.7%		213.6615	0	0.050872
26	211.46	7.27	-46.37	1885.0%		211.5874	0	0.050378
27	209.39	7.27	-46.37	1904.6%		209.5133	0	0.049884
28	207.31	7.27	-46.37	1924.7%		207.4393	0	0.04939
Sum	5950.00	0.00	0.00					

Table A.3 - 10-G Vertical Load – Superposition Solution

ATTACH	X REACT	Y REACT	Z REACT	MS		shear	Rt	Rs
1	0.00	0.00	100.23	4390%		0	0.022272	0
2	0.00	0.00	89.90	4905%		0	0.019978	0
3	0.00	0.00	79.58	5555%		0	0.017684	0
4	0.00	0.00	69.25	6398%		0	0.015389	0
5	0.00	0.00	58.93	7536%		0	0.013095	0
6	0.00	0.00	48.60	9159%		0	0.010801	0
7	0.00	0.00	38.28	11656%		0	0.008507	0
8	0.00	0.00	27.95	15997%		0	0.006212	0
9	0.00	0.00	17.63	25424%		0	0.003918	0
10	0.00	0.00	10.53	42625%		0	0.002341	0
11	0.00	0.00	3.43	130931%		0	0.000763	0
12	0.00	0.00	107.49	4086%		0	0.023887	0
13	0.00	0.00	96.91	4543%		0	0.021536	0
14	0.00	0.00	86.33	5112%		0	0.019185	0
15	0.00	0.00	75.75	5840%		0	0.016834	0
16	0.00	0.00	65.17	6805%		0	0.014483	0
17	0.00	0.00	54.59	8143%		0	0.012132	0
18	0.00	0.00	44.01	10124%		0	0.009781	0
19	0.00	0.00	33.43	13359%		0	0.00743	0
20	0.00	0.00	22.86	19589%		0	0.005079	0
21	0.00	0.00	15.58	28780%		0	0.003463	0
22	0.00	0.00	8.31	54064%		0	0.001846	0
23	0.00	0.00	7.64	58774%		0	0.001699	0
24	0.00	0.00	6.93	64792%		0	0.001541	0
25	0.00	0.00	6.23	72182%		0	0.001383	0
26	0.00	0.00	5.52	81470%		0	0.001226	0
27	0.00	0.00	4.81	93497%		0	0.001068	0
28	0.00	0.00	4.10	109685%		0	0.000911	0
Sum	0.00	0.00	1190.00					